Comparative Biochemistry and Physiology, Part A 157 (2010) 328–337

Contents lists available at ScienceDirect

Comparative Biochemistry and Physiology, Part A

journal homepage: www.elsevier.com/locate/cbpa

Myostatin from the American lobster, *Homarus americanus*: Cloning and effects of molting on expression in skeletal muscles

Kyle S. MacLea [a], Joseph A. Covi [a], Hyun-Woo Kim [a], Erica Chao [a], Scott Medler [a], Ernest S. Chang [b], Donald L. Mykles [a,*]

[a] Department of Biology, Colorado State University, Fort Collins, CO 80523, USA
[b] Bodega Marine Laboratory, University of California-Davis, Bodega Bay, CA 94923, USA

ARTICLE INFO

Article history:
Received 18 May 2010
Received in revised form 27 July 2010
Accepted 30 July 2010
Available online 7 August 2010

Keywords:
Myostatin
Gene expression
Crustacea
Arthropoda
Ecdysteroid
Molting
mRNA
Skeletal muscle
Eyestalk ablation
Tissue distribution
cDNA cloning
DNA sequence
Amino acid sequence

ABSTRACT

A cDNA encoding a myostatin (Mstn)-like gene from an astacuran crustacean, *Homarus americanus*, was cloned and characterized. Mstn inhibits skeletal muscle growth in vertebrates and may play a role in crustacean muscle as a suppressor of protein synthesis. Sequence analysis and three-dimensional modeling of the Ha-Mstn protein predicted a high degree of conservation with vertebrate and other invertebrate myostatins. Qualitative polymerase chain reaction (PCR) demonstrated ubiquitous expression of transcript in all tissues, including skeletal muscles. Quantitative PCR analysis was used to determine the effects of natural molting and eyestalk ablation (ESA) on Ha-Mstn expression in the cutter claw (CT) and crusher claw (CR) closer muscles and deep abdominal (DA) muscle. In intermolt lobsters, the Ha-Mstn mRNA level in the DA muscle was significantly lower than the mRNA levels in the CT and CR muscles. Spontaneous molting decreased Ha-Mstn mRNA during premolt, with the CR muscle, which is composed of slow-twitch (S_1) fibers, responding preferentially (82% decrease) to the atrophic signal compared to fast fibers in CT (51% decrease) and DA (69% decrease) muscles. However, acute increases in circulating ecdysteroids caused by ESA had no effect on Ha-Mstn mRNA levels in the three muscles. These data indicate that the transcription of Ha-Mstn is differentially regulated during the natural molt cycle and it is an important regulator of protein turnover in molt-induced claw muscle atrophy.

1. Introduction

Myostatin (Mstn), a member of the TGF-β superfamily of cytokines, is a critical autocrine/paracrine inhibitor of muscle growth in vertebrates (Lee, 2004; Lee and McPherron, 2001; McPherron et al., 1997; Rodgers and Garikipati, 2008). Indeed, so-called "double-muscled" breeds of cattle and sheep (Hadjipavlou et al., 2008; McPherron and Lee, 1997) have point mutations in their Mstn genes, leading to inactive gene products unable to restrain muscle growth. Experiments in other higher vertebrate species, including mouse, pig, dog, and chicken, show similar effects on muscle mass (McPherron and Lee, 1997; Mosher et al., 2007; Patruno et al., 2008; Welle et al., 2009; Ye et al., 2007). This function is also conserved in lower vertebrates, including fish (Medeiros et al., 2009). Mstn signaling is mediated by activin membrane receptors, resulting in the activation of Smad transcription factors (reviewed by Kollias and McDermott, 2008). Mstn acts, at least in mammals, by simultaneously suppressing protein synthesis and stimulating protein degradation, which leads to reduction in skeletal muscle mass associated with disuse, aging, and disease in adults (reviewed by Matsakas and Patel, 2009; Tisdale, 2009).

Recently, the identification of Mstn-like genes in arthropods and mollusks has prompted investigations of their function(s), especially with regard to their ability to regulate growth of muscle in invertebrates. cDNAs encoding Mstn-like proteins have been characterized from fruit fly, *Drosophila melanogaster* (designated myoglianin; Lo and Frasch, 1999), bay scallop, *Argopecten irradians* (Ai-Mstn; Kim et al., 2004), Chinese mitten crab, *Eriocheir sinensis* (Es-Mstn; Kim et al., 2009), and blackback land crab, *Gecarcinus lateralis* (Gl-Mstn; Covi et al., 2008). The domain organization of the deduced protein sequences is highly conserved, consisting of N-terminal signal peptide, propeptide, and mature peptide domains; the furin cleavage site between the propeptide and mature peptide domains is also conserved (Covi et al., 2008; Kim et al., 2004, 2009; Lo and Frasch, 1999). All invertebrate Mstn-like proteins have the nine conserved cysteine residues that participate in intramolecular and intermolecular disulfide bonding in the native homodimer (Covi et al., 2008; Kim et al., 2004, 2009; Lo

* Corresponding author. Tel.: +1 970 491 7616; fax: +1 970 491 0649.
E-mail address: don@lamar.colostate.edu (D.L. Mykles).

1095-6433/$ – see front matter © 2010 Elsevier Inc. All rights reserved.
doi:10.1016/j.cbpa.2010.07.024

and Frasch, 1999). The arthropod Mstn is expressed in skeletal muscle, heart, and various non-muscle tissues, which suggest it has functions not restricted to limiting skeletal muscle mass (Covi et al., 2008; Kim et al., 2009; Lo and Frasch, 1999).

The skeletal muscle of decapod crustaceans, such as crabs and lobsters, is highly plastic and able to undergo dramatic remodeling associated with development and growth (reviewed by Govind, 1992; Mykles, 1997; Mykles and Skinner, 1982a). The reversible atrophy of the claw muscles seen during the preparation for ecdysis, or molting, is a critical process enabling the withdrawal of the large closer muscle through the comparatively narrow basi-ischial joint when the old exoskeleton is shed (reviewed by Mykles, 1997). In land crab during the premolt period (~4 weeks), as much as 78% of the muscle mass is reduced (Mykles and Skinner, 1982a; Skinner, 1966). A similar molt-induced atrophy occurs in the claw muscles of fiddler crab, *Uca pugilator* (Ismail and Mykles, 1992), and crayfish, *Cherax destructor* (West, 1997). This atrophy is specific to the claws and does not occur in thoracic or leg muscles (Griffis et al., 2001; Mykles and Skinner, 1982a; Schmiege et al., 1992). After ecdysis, the muscle grows to fill the available space (Medler et al., 2007; Skinner, 1966).

In the land crab, Gl-Mstn expression and protein turnover in skeletal muscle is regulated during the molt cycle. The transcript abundance of Gl-Mstn is reduced in both the claw and thoracic muscles during premolt (Covi et al., 2010). However, the decrease is about 3 times greater in claw muscle than in the thoracic muscle (Covi et al., 2010). The down regulation of Gl-Mstn expression in the claw muscle coincides with 11- and 13-fold increases in protein synthesis in the myofibrillar and soluble protein fractions, respectively (Covi et al., 2010; Skinner, 1965). This global increase in protein synthesis appears counterproductive, as an even greater increase in protein degradation is required to effect the reduction in muscle mass that occurs (Mykles and Skinner, 1981; Skinner, 1966). The accelerated protein turnover may facilitate an extensive remodeling of the myofibrils that coincides with muscle atrophy (Mykles, 1997). Coincident with a reduction in myofibrillar cross-sectional area, there is a preferential elimination of thin myofilaments, which results in a decrease in the thin:thick myofilament ratio from ~9:1 to ~6:1 and an increase in thick myofilament packing between 51% and 72% (Ismail and Mykles, 1992; Mykles and Skinner, 1981, 1982b). These data suggest that, like mammalian Mstn, Gl-Mstn is a suppressor of protein synthesis.

The effects of Mstn depend on the fiber type composition of skeletal muscles. In mammals, Mstn preferentially acts on the fast fibers and may influence the fiber type composition of skeletal muscle (reviewed by Kollias and McDermott, 2008). Mstn is expressed at higher levels in the fast glycolytic (type IIb) fibers than in the slow oxidative (type I) fibers (Carlson et al., 1999; Salerno et al., 2004). Moreover, the amount of activin IIB receptor protein is greater in fast muscle than in slow muscle (Mendias et al., 2006). Down regulation of Mstn results in a developmental shift from slow to type IIb fibers (Girgenrath et al., 2005; Hennebry et al., 2009; Steelman et al., 2006). These data indicate that fast fibers, specifically type IIb, are more sensitive to Mstn. Indeed, type IIb fibers hypertrophy to a greater extent than type I and IIa fibers in Mstn knockout mice (Mendias et al., 2006) and in adult mice in which Mstn is inhibited by the over-expression of Mstn propeptide (Foster et al., 2009; Matsakas et al., 2009).

Fiber phenotype may play a role in the differential sensitivity of crustacean muscles to molt-induced atrophy. In the claw closer muscles of land and fiddler crabs, slow-twitch (S_1) fibers undergo a greater atrophy than slow-tonic (S_2) fibers (Ismail and Mykles, 1992; Mykles, 1997). The American lobster, *H. americanus*, has dimorphic claws that differ in size, morphology, and fiber composition (reviewed by Govind, 1992; Mykles, 1997). The larger "crusher" claw closer muscle consists entirely of slow-twitch (S_1) fibers, while the more slender "cutter" claw closer consists mostly of fast, some S_1, and a small population of slow-tonic (S_2) fibers (Medler et al., 2007; Medler and Mykles, 2003; Mykles, 1985). In his monograph on the American lobster, Herrick (1895) recognized the mechanical problem of pulling the claws through the narrow joints at ecdysis. Given the larger mass of the crusher claw (Herrick, 1895), we hypothesize that the fibers in the crusher undergo a greater atrophy than the fibers in the cutter claw. Consequently, the fast and S_1 fiber types may differ in Mstn expression in response to the elevated ecdysteroids associated with molting.

Here we report the cloning and characterization of a cDNA encoding the partial sequence of an Mstn-like protein in *H. americanus* (Ha-Mstn). The tissue distribution of Ha-Mstn mRNA was determined by end-point polymerase chain reaction (PCR). The effects of molting on Ha-Mstn expression in fast fibers in cutter claw closer and deep abdominal muscles and S_1 fibers in the crusher claw closer were determined by quantitative PCR (qPCR).

2. Materials and methods

2.1. Animals and experimental treatments

Adult lobsters, *H. americanus*, both males and females, were raised from larvae in the culture facility at Bodega Marine Laboratory (Chang and Conklin, 1983; Conklin and Chang, 1983). Animals were maintained at ambient temperatures (12–16 °C) and fed with shrimp or squid once a week. For the eyestalk ablation experiment, lobsters had both eyestalks ablated at the base with scissors and then the animals were maintained for 7 or 22 days before they were sacrificed ($n=3$ for each time point). Animals from the same age group ($n=6$) were left with eyestalks intact and served as intact controls. Muscles from the cutter (CT) and crusher (CR) claws, as well as from the deep abdominal (DA) flexor muscles, were frozen in liquid nitrogen and then stored at −80 °C until processing for RNA isolation. Hemolymph samples (0.1 mL) were taken at the time of sacrifice, drawn from the arthrodial membrane at the base of the last pair of walking legs with a 1-mL syringe fitted with a 26-gauge needle and combined with 0.3 mL methanol. Ecdysteroid levels in the hemolymph were quantified by radioimmunoassay as described previously (Chang and O'Connor, 1979; Yu et al., 2002).

A second experiment evaluated lobsters at different stages of the natural molt cycle. Animals at intermolt ($n=4$), late premolt ($n=3$), or postmolt stages ($n=4$) were collected. Molt staging was based on a combination of molt record, hemolymph ecdysteroid concentration, exoskeletal structure, and/or pleopod setal development (Aiken, 1973). Premolt animals were determined to be at stage D_{1-2}. Intermolt (stage C_4) animals were identified by the presence of a membranous layer in the exoskeleton. Postmolt animals (stage B) were identified on the basis of when molts were recorded for each animal. Hemolymph samples from premolt animals and muscle tissues were processed as described above.

2.2. RNA purification and cDNA synthesis

Total RNA was isolated from lobster tissues using TRIzol reagent (Life Technologies, Carlsbad, CA) as described previously (Covi et al., 2010). Briefly, tissues (50–200 mg) were homogenized in 1–2 mL TRIzol and centrifuged at 12,000 *g* for 15 min at 4 °C. Supernatants were phenol–chloroform extracted and RNA in the aqueous phase was precipitated using isopropanol (0.75 mL per 1 mL TRIzol reagent). RNA was treated with DNase I (Fermentas, Glen Burnie, MD, USA), extracted twice with phenol:chloroform:isoamyl alcohol (25:24:1), precipitated with isopropanol, washed twice with 75% ethanol in DEPC water, and resuspended in nuclease-free water. First-strand cDNA was synthesized using 1 μg total RNA in a 20 μL total reaction with SuperScript III reverse transcriptase (Life Technologies) and oligo-dT(20)VN primer (50 μmol/L) as described (Covi et al., 2010).

RNA was treated with RNase H (Fisher Scientific, Pittsburgh, PA, USA) and stored at −80 °C.

2.3. Cloning of the lobster myostatin gene

RT-PCR and RACE were used to clone the Ha-Mstn cDNA. Total RNA was isolated from CT, CR, and DA muscles and cDNA was synthesized as above. PCR was conducted using 0.5 μL first-strand cDNA as template with forward (10 pmol) and reverse (10 pmol) primers (F51 and R51; Table 1) directed against the green crab (*Carcinus maenas*) Mstn sequence (unpublished data). PCR reactions used GoTaq Green master mix (Promega, Madison, WI, USA). After denaturing the cDNA at 96 °C for 3 min, 35 cycles of PCR were completed with the following program: 96 °C for 30 s, 62 °C for 30 s, and 72 °C for 1 min. Final extension was for 7 min at 72 °C. Amplified fragments from DA and CR muscles, verified as single bands by 1% agarose gel electrophoresis, were purified using the GeneJet PCR Cloning Kit (Fermentas), ligated into the pJET1.2 vector using the CloneJet PCR Cloning Kit (Fermentas), and, after insert verification by PCR with vector primers, sequenced using a T7 primer (Davis Sequencing, Davis, CA, USA).

The FirstChoice RLM-RACE Kit (Applied Biosystems, Austin, TX, USA) was used according to the manufacturer's instructions to amplify additional parts of the coding sequence using nested 5′ and 3′ RACE and various primers shown in Table 1. RACE conditions were as follows: 0.4 μL RACE template cDNA was used in each reaction, with 8 pmol of each gene-specific (Table 1) and kit primer, and other components identical to the initial PCR reactions (see above). After denaturation at 94 °C for 3 min, 35 cycles of 94 °C for 30 s, annealing temperature (Table 1) for 30 s, and 72 °C for 30 s, were completed. Final extension was for 7 min at 72 °C. All products were cloned and sequenced as described above.

In addition to RACE, additional 5′ sequence was obtained using nested primers. cDNA template from mixed tissues (1 μL) was used in each reaction, with 10 pmol degenerate forward primers and 5 pmol gene-specific reverse primers. PCR conditions were the same as for RACE, above, but used different annealing temperatures and 72 °C extension time (Table 1), depending on the primer combination. The annealing temperature used the lower temperature of a primer pair (Table 1).

2.4. Tissue expression and quantification of Ha-EF2 and Ha-Mstn mRNAs

End-point PCR was used to qualitatively assess the tissue distribution of Ha-Mstn (GenBank GU989035) and Ha-EF2 (GenBank FJ790217; Chao et al., 2010) transcripts. Total RNA was purified from tissues of an intermolt female adult lobster as described above. Reactions contained 1 μL template cDNA and 5 pmol each of the Ha-Mstn or Ha-EF2 expression primers (Table 1) in GoTaq Green master mix (Promega). After denaturation at 94 °C for 3 min, 29 cycles (Ha-Mstn) or 30 cycles (Ha-EF2) of 94 °C for 30 s, 60 °C (Ha-Mstn) or 62 °C (Ha-EF2) for 30 s, and 72 °C for 30 s, were completed. Final extension was for 7 min at 72 °C. After PCR was terminated, products were separated on a 1% agarose gel containing TAE (40 mM Tris acetate and 2 mM EDTA, pH 8.5). Representative gels (of 3 replicates) were stained with ethidium bromide and visualized with a UV light source.

A LightCycler 480 thermal cycler (Roche Applied Science, Indianapolis, IN) was used to quantify levels of Ha-Mstn and Ha-EF2 mRNAs. Reactions consisted of 1 μL first-strand cDNA or standard, 5 μL 2×SYBR Green I Master mix (Roche Applied Science), 0.5 μL each of 10 mM forward and reverse primers (Table 1), and 3 μL nuclease-free water. PCR conditions were as follows: an initial denaturation at 95 °C for 5 min, followed by 45 cycles of denaturation at 95 °C for 10 s, annealing at 62 °C for 20 s, and extensions at 72 °C for 20 s, followed by the melting curve analysis of the PCR product. Transcript concentrations were determined by use of the LightCycler 480 software (Roche, version 1.5) using a series of dsDNA gene standards produced by serial dilutions of PCR product for each gene (10 ag/μL to 10 ng/μL). The absolute amounts of transcript in copy numbers per μg of total RNA in the cDNA synthesis reaction were calculated based on the standard curve and the calculated molecular weight of dsDNA products of Ha-Mstn and Ha-EF2. Ha-Mstn transcript copy numbers were normalized according to the internal control Ha-EF2 copy numbers per μg total RNA observed in each sample as follows. After verifying that there was no statistical difference in the observed means of the Ha-EF2 levels by muscle type or experimental treatment, the Ha-EF2 copy number per μg of total RNA for each sample cDNA was divided by the average Ha-EF2 copy number per μg of total RNA for all samples tested in the experiment. The mean ± 1 S.E. was $4.46 \pm 0.49 \times 10^7$ ($n = 57$). Transcript copy numbers, computed for each sample based on the standard curve for Ha-Mstn, were then divided by this ratio to normalize Mstn expression to Ha-EF2 in the different samples.

2.5. Statistical analyses and software

Statistical analysis was performed using JMP 8.0.2 (SAS Institute, Cary, NC). Group variances were analyzed using a Brown–Forsythe test and found to be equal ($P<0.05$). Means for different

Table 1
Oligonucleotide primers used in the cloning or expression analysis of lobster myostatin (Ha-Mstn; GenBank GU989035) and expression analysis of lobster elongation factor 2 (Ha-EF2; FJ790217).

Primer	Sequence (5′-3′)	Position in cDNA	Application	Anneal Temp/Ext Time
F51	CGCCCACAAGTACGCCCACA	745–764	I, E, 3′ (outer)	62 °C (60 °C)
R51	GCAGCCGCAGCGGTCTACTACC	919–898	I, E	62 °C
3′ RACE F1	GCTCGTCCAGAAGTTGAACAGC	769–790	3′ (outer and inner)	59 °C
3′ RACE F2	GAACAGCAGCAACGCCCATC	784–803	3′ (inner)	59 °C
5′ RACE R4	CGTACTTGTGGGCGTACAGGA	758–738	5′ (outer)	58 °C
5′ RACE R3	TCACCGTTACAGAAGTTGGCT	729–709	5′ (inner)	58 °C
Ha-Mstn F3	GAYGARCCNGANGTNAARACN	100–121	A (outer)	44 °C (1.25 min)
Ha-Mstn F4	CCNGARGGNACNGAYGTN	170–187	A (inner)	44 °C (1.25 min)
Ha-Mstn R1	TTCTGGTGGTATGCGGAGTCC	178–158	A (inner)	44 °C (1.25 min)
Ha-Mstn R4	TGAGTCGTAGGCAGTCACCAC	484–464	A (outer)	44 °C (1.25 min)
Ha-Mstn F1	AMYCCHCCHAAYATGACHGG	−20–0	A (outer and inner)	45 °C (1 min)
Ha-Mstn F2	GTNCARGGHATYATYGA	28–45	A (inner)	40 °C (1 min)
Ha-Mstn R3	ATGGTCATGGTCGTAGTA	868–851	A (outer and inner)	45 °C, 40 °C (1 min)
Ha-EF2 F1	TTCTATGCCTTCGGACGTGTGTTCTC	1252–1277	E	62 °C
Ha-EF2 R1	TGATGGTGCCAGTCTTGACCAGGTAC	1480–1455	E	62 °C

*Abbreviations: A, primers used for additional 5′ sequence amplification by RT-PCR; E, primer used for expression analysis by RT-PCR; I, primer used for initial amplification by RT-PCR; 3′, primer used for 3′ RACE (inner or outer) PCR; 5′, and primer used for 5′ RACE PCR.

developmental stages were compared using analysis of variance (ANOVA). All data not plotted as individual points are represented as mean ± 1 S.E. and the level of significance was set at $\alpha = 0.05$. Linear regression analysis of log-transformed data was performed using Excel 2007 (Microsoft, Redmond, WA) and JMP 8.0.2. The slopes of each regression line were compared with $y = 0$ by ANOVA and p-values are reported in the relevant figures and text. Grapher 8.2.460 (Golden Software, Golden, CO), Excel, and Illustrator 10 (Adobe Systems, San Jose, CA) were used for constructing graphs.

Multiple sequence alignments were produced with ClustalX version 2.0.12 (Thompson et al., 1997) using deduced amino acid sequences. The phylogenetic tree was derived using the neighbor-joining method and visualized as a rooted dendrogram with the *D. melanogaster* decapentaplegic MP sequence as the outgroup and indicated relative branch lengths using TreeView version 1.6.6 (Page, 1996). Bootstrap values are indicated at each node, computed by ClustalX. Illustrator 10 was used to annotate the images derived from these analyses.

3. Results

3.1. Cloning and characterization of lobster Mstn-like cDNA

Using RT-PCR and RACE, a partial cDNA encoding Mstn from the American lobster, *H. americanus*, was isolated and characterized. We were unable to clone the 5′ end of the gene, despite numerous attempts with 5′ RACE, degenerate RT-PCR, and other techniques (e.g., inverse PCR, genome walking, genomic DNA degenerate PCR cloning, and cDNA library degenerate PCR cloning). The cDNA (1314 nucleotides or nt) coded for about half of the propeptide region, the complete mature peptide (MP; 112 amino acids) sequence, and complete 3′ UTR (Fig. 1). The furin proteolytic site (RXXR) was present, which is consistent with the processing of MPs of other TGF-β family members (Herpin et al., 2004; Lee, 2004). The 3′ UTR contained 8 putative polyadenylation (poly A) signal sequences, including a GTTAAA sequence (MacDonald and Redondo, 2002) located within 50 nt of the poly A tract (Fig. 1).

The partial cDNA, when translated, showed the greatest identity to the two decapod crustacean Mstn cDNAs cloned from *G. lateralis* (Gl-Mstn; GenBank ACB98643; 71% identity/80% similarity) and *E. sinensis* (Es-Mstn; ACF40953; 59%/72%) (Covi et al., 2008; Kim et al., 2009). Fig. 2 compares the two complete crab sequences with the lobster partial sequence and myostatin sequences from an insect (Tc-Mstn) and human (Hs-Mstn). In the multiple sequence alignment, the RXXR furin cleavage site is indicated (box), along with the 9 cysteines (indicated with arrows) conserved in all Mstn and inhibin/activin-like TGF-β family members. The homology seen among the decapod myostatins becomes even more pronounced when only the mature peptide is examined. Then, the identity and similarity increased to 87%/91% for *G. lateralis* and 81%/91% for *E. sinensis*.

BLAST analysis showed that the Ha-Mstn was most similar to Mstn-like factors within the TGF-β family. The top ~50 hits when the clone was searched by the translated protein sequence were all for Mstn or GDF-8-like genes, with other members of the TGF-β family having lower

```
agtagtgatatctcaaaatccaaacatccaggggattatagaagaaatgcggacgtcggta   61
 V  V  I  S  Q  N  P  N  I  Q  G  I  I  E  E  M  R  T  S  V    20
cctcagacagcctacatgcaggagcctccgtacaatgacgacgagccagagagcaagaca  121
 P  Q  T  A  Y  M  Q  E  P  P  Y  N  D  D  E  P  E  S  K  T    40
gagaagatgttctcccccgtagaaccagcacccccggactccgcataccaccagaaata  181
 E  K  M  F  S  P  V  E  P  A  P  P  G  L  R  I  P  P  E  I    60
gacgtgctctactttaaactaaaccacgagcagctggggaaccgggtgaagagagccatc  241
 D  V  L  Y  F  K  L  N  H  E  Q  L  G  N  R  V  K  R  A  I    80
ctccacgtctggctcaaacctatgcactccgagctggaccgcaccgtgcccatcactgta  301
 L  H  V  W  L  K  P  M  H  S  E  L  D  R  T  V  P  I  T  V   100
tacaaggtgtcaaggcccgagagtttgggcggcttcatcaggaccaatgaggtgacgacg  361
 Y  K  V  S  R  P  E  S  L  G  G  F  I  R  T  N  E  V  T  T   120
gtatctgaatccttcgacgctcggaaaggtaactgggtgaagatcgaagtgtacaagtta  421
 V  S  E  S  F  D  A  R  K  G  N  W  V  K  I  E  V  Y  K  L   140
ctacaagagtggctcaataaacccaacgacaacctggggctggtggtgactgcctacgac  481
 L  Q  E  W  L  N  K  P  N  D  N  L  G  L  V  V  T  A  Y  D   160
tcacagggtagacaagtggccgtcaccgaccccaatgagatgccttctaacgcgccgcta  541
 S  Q  G  R  Q  V  A  V  T  D  P  N  E  M  P  S  N  A  P  L   180
ctggagatccacacggaggagacgaggaagagtcggtctcgacgtaacagtggcaacaac  601
 L  E  I  H  T  E  E  T  R  K  S  R  S  R  R  N  S  G  N  N   200
ttcttctgcaccaacaacaagaaggagtcgcgctgttgtcgctatcaactcgtcgtcaac  661
 F  F  C  T  N  N  K  K  E  S  R  C  C  R  Y  Q  L  V  V  N   220
tttatcgagttaggttgggacttcatcgtcgcccccaagacatacgaagccaacttctgt  721
 F  I  E  L  G  W  D  F  I  V  A  P  K  T  Y  E  A  N  F  C   240
aacggtgaatgccccttcctgtacgcccacaagtacgcccacacctcgctcgtccagaag  781
 N  G  E  C  P  F  L  Y  A  H  K  Y  A  H  T  S  L  V  Q  K   260
ttgaacagcagcaacgcccatcacggcccttgttgcggcgccaggaagctgtcgcccatg  841
 L  N  S  S  N  A  H  H  G  P  C  C  G  A  R  K  L  S  P  M   280
aagatgctctactacgaccatgaccataaaatcaaatttgataccatccaagacatggta  901
 K  M  L  Y  Y  D  H  D  H  K  I  K  F  D  T  I  Q  D  M  V   300
gtagaccgctgcggctgctcctaagcctatgctaggtatccactactaaaccgttctttc  961
 V  D  R  C  G  C  S  *                                       307

caataaagatctgtgatggagagtagatttaaattgggctcgtattccagtgtccagtcc 1021
aaacacaatttgtaaacgttgttattgttccctgtaaatactgaacaaaaatcctttta 1081
atatcaatgcaatttataactaaagtatctcactcttatgtttacgaagtaagagttatt 1141
acacgccactactcagtcaactagcggcctggcggaagtgttgtgcgctgttctctctag 1201
aggcaaaactaaaaatttaaacgccgtgatttttttgtgtagatatttagttacacggct 1261
ggttaaaatctccatacattagaaaaaaaaaaaaaaaaaaaaaaaaaaaaaaaaaaaa   1314
```

Fig. 1. Partial nucleotide and amino acid sequences including incomplete open read frame and 3′ untranslated region (UTR) of the *H. americanus* myostatin (GenBank accession GU989035). The RSRR furin/subtilisin cleavage site is boxed with the resulting mature peptide amino acid sequence shown in bold and italics. The stop codon is indicated with an asterisk. Putative polyadenylation signals in the 3′ UTR are in bold and underlined.

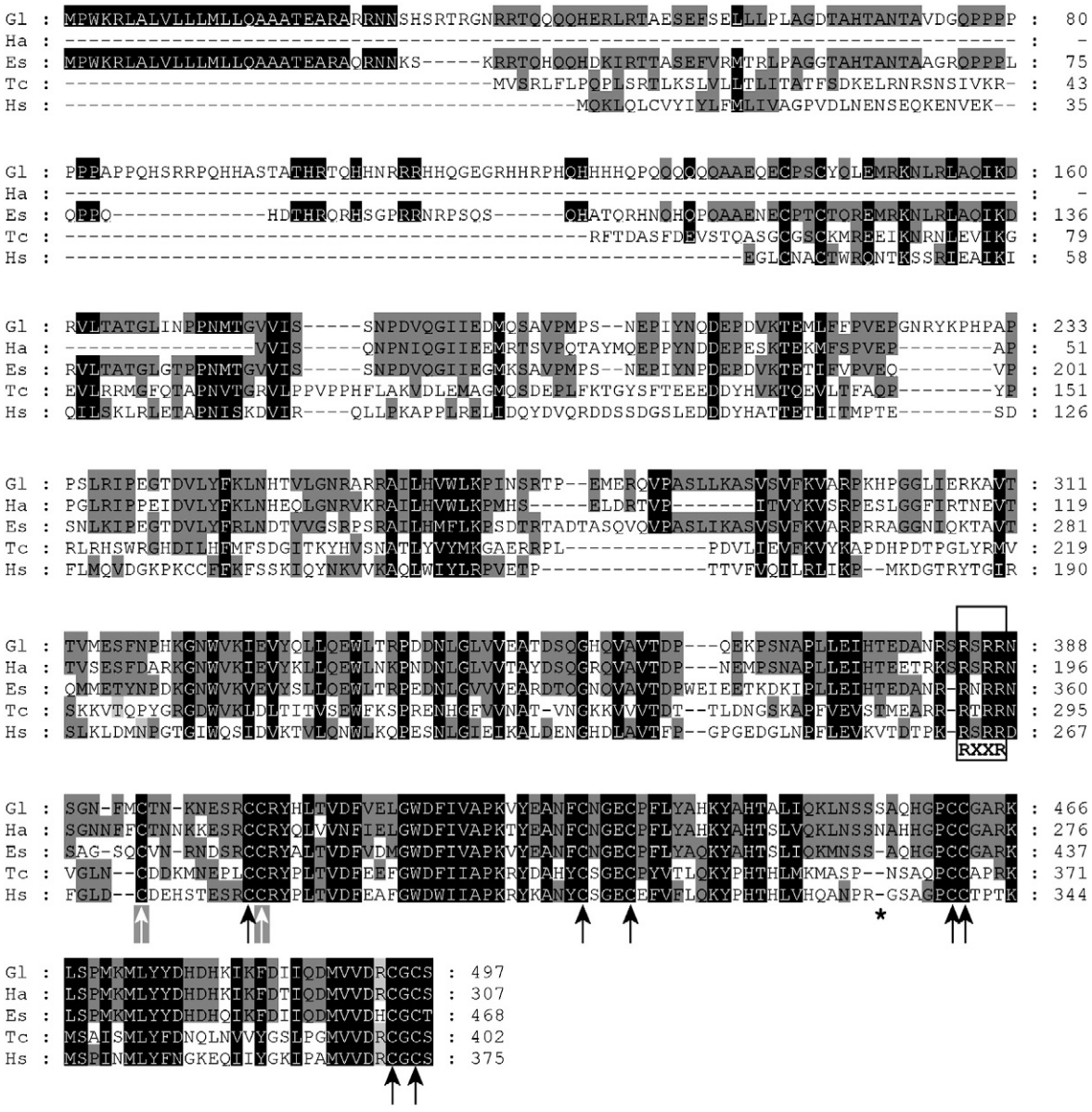

Fig. 2. Multiple alignment of deduced amino acid sequences for myostatin-like proteins from crustaceans, an insect, and human. Abbreviations: blackback land crab, *G. lateralis* (Gl; GenBank ACB98643; Covi et al., 2008), American lobster, *H. americanus* (Ha; GU989035; partial sequence, this study), Chinese mitten crab, *E. sinensis* (Es; ACF40953; Kim et al., 2009); red flour beetle, *Tribolium castaneum* (Tc; XP_966819); and human, *Homo sapiens* (Hs, NP_005250). The Gl- and Ha-Mstn sequences are 71% identical and 80% similar to each other, while Es- and Ha-Mstn are 59% identical and 72% similar. Arrows below the alignment indicate the seven cysteines present in all TGF-β family members (black arrows) and two additional cysteines present in inhibin/activin and myostatin-like members of the family (white arrows on gray background). The predicted furin/subtilisin cleavage site (RXXR) is indicated with a box. Dashes indicate gaps introduced to optimize the alignment. Asterisk (*) indicates the loop region with structural divergence indicated with an arrow in Fig. 7A.

similarity scores. This confirmed the analysis completed for the Gl-Mstn (Covi et al., 2008). The result of a phylogenetic comparison of the 112-amino acid MP from *H. americanus* with vertebrate and invertebrate TGF-β MPs (Mstn-, BMP-, and activin-like) is shown in Fig. 3. The boxed portion of the phylogenetic tree shows the Ha-Mstn sequence grouping with Mstn sequences from other decapod crustaceans (*G. lateralis*, *E. sinensis*, and *Litopenaeus vannamei*). Searches of sequence databases identified a previously uncharacterized EST encoding a Mstn-like protein from Pacific white shrimp (*L. vannamei*). The Lv-Mstn EST sequence (FE135924; 625 bp) encodes the MP (115 amino acids), a small portion of the PP (22 amino acids), and 214 bp of 3′UTR, with its strongest BLAST match to *G. lateralis* Mstn (81% identity/89% similarity). More phylogenetically distant invertebrates were more divergent. The overall degree of similarity in the MP region was high among all the invertebrate myostatins. Ha-Mstn also showed 50%/68% identity/similarity to the human sequence within this region, with large sections showing complete identity. For example, the last 9 amino acids (MVVDRCGCS) were completely identical in the lobster, land crab, red flour beetle, and human myostatins, underscoring the homology of Ha-Mstn with these sequences.

RT-PCR was used to amplify Mstn and EF2 transcripts from several tissues of an adult female lobster (Fig. 4, representative image of 3 RT-PCR replicates). Ha-Mstn was expressed at various levels in all eleven tissues, with apparently higher levels in deep abdominal (DA) muscle and hindgut (HG), moderate levels in the crusher claw closer muscle (CR), hepatopancreas (HP), thoracic ganglia (TG), and midgut (MG), lower levels in the cutter claw closer (CT) and superficial abdominal (SA) muscles and the antennal gland (AG), with even lower levels seen in the ovary (O) and lowest expression in the heart (H). Ha-EF2 was expressed at similar levels in all tissues.

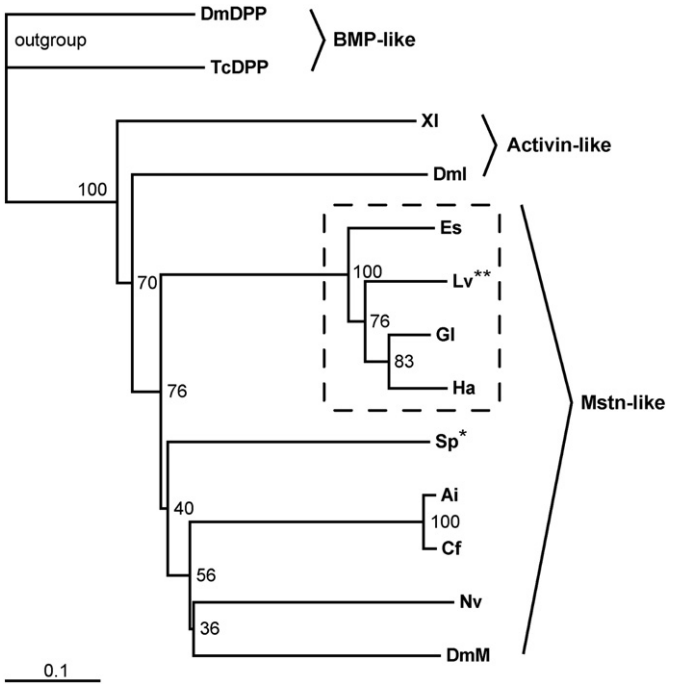

Fig. 3. Phylogenetic analysis of vertebrate and invertebrate myostatin-like proteins compared with other TGF-β family members. The deduced mature peptide sequences were used to construct the tree and bootstrap values are indicated at each node; decapentaplegic (DPP) served as the outgroup. All the decapod crustacean myostatins clustered as a group, as indicated by the box with dashed line. Mstn-like proteins in other invertebrates were more closely related to the decapod crustacean sequences than to sequences from activin-like or BMP-like TGF-β protein sequences. Abbreviations: Ai, *A. irradians* (bay scallop; AAT36326); Cf, *Chlamys farreri* (Zhikong scallop; ACB87200); DmDPP, *D. melanogaster* decapentaplegic (P07713); Dml, *D. melanogaster* inhibin beta chain (O61643); DmM, *D. melanogaster* myoglianin (AAD24472); Es, *E. sinensis* (Chinese mitten crab; ACF40953); Gl, *G. lateralis* (blackback land crab; ACB98643); Ha, *H. americanus*, (American lobster; GU989035); Lv, *Litopenaeus vannamei* (Pacific white shrimp; FE135924); Nv, *Nematostella vectensis* (starlet sea anemone; XP001641598); Sp, *Strongylocentrotus purpuratus* (purple sea urchin; XP789990); TcDPP, *T. castaneum* decapentaplegic (red flour beetle; Q26974); and Xl, *Xenopus laevis* activin D (African clawed frog; BAA08494). Asterisk (*) indicates sequences predicted from genomic data; all other sequences originate from cDNA. Double asterisk (**) indicates sequences derived from previously uncharacterized ESTs. Scale represents proportion of amino acid differences between sequences based on nucleotide substitutions per site.

3.2. Effects of molting on expression of Ha-EF2 and Ha-Mstn

Quantitative PCR was used to analyze levels of Ha-Mstn in the fast fibers in the CT closer muscle, the S_1 fibers in the CR closer muscle, and the fast fibers in the DA muscle, as animals progressed through a natural molt cycle (Fig. 5). Animals at three molt stages were examined: intermolt (anecdysis or stage C_4; INT), late premolt (stages D_1–D_2; PRE; hemolymph ecdysteroid = 180.6 ± 53.0 pg/μL, n = 3), and postmolt (stage B; POST). Hemolymph ecdysteroid was not measured at INT and POST stages, but previous work shows that the levels are low (<35 pg/μL) at these stages (Chang and Bruce, 1980). There was a small variation in Ha-EF2 mRNA levels (1.7–to 2.3-fold) between the molt stages, but no statistically significant differences in the means were observed. The Ha-EF2 mRNA levels (transcript copy number/μg total RNA) were: $3.60 \pm 0.93 \times 10^7$ for INT CR, $8.62 \pm 1.99 \times 10^7$ for PRE CR, and $3.84 \pm 1.84 \times 10^7$ for POST CR; $4.76 \pm 1.36 \times 10^7$ for INT CT, $9.11 \pm 4.39 \times 10^7$ for PRE CT, and $3.66 \pm 1.76 \times 10^7$ for POST CT; and $4.99 \pm 0.78 \times 10^7$ for INT DA, $1.07 \pm 0.34 \times 10^7$ for PRE DA, and $4.09 \pm 2.21 \times 10^7$ for POST DA). However, to ensure that these small differences in Ha-EF2 did not affect the interpretation of the data, the Ha-Mstn qPCR results were normalized relative to the average Ha-EF2 expression in all samples (see Materials and methods). Statistical differences were observed in the expression of Ha-Mstn in the muscle tissues (Fig. 5). Progressing from intermolt to premolt, CR and DA muscles both showed significant decreases in expression of Ha-Mstn. CR muscle expression decreased 82% in premolt, while DA decreased 69%. The mean Ha-Mstn mRNA level in the CT muscle from premolt animals was 51% lower than the mRNA level at intermolt, but the means were not significantly different ($p = 0.069$). There were no significant differences in the Ha-Mstn mRNA levels between postmolt and premolt stages in all three muscles, which were probably due to the greater variability in the Ha-Mstn mRNA levels in postmolt animals.

Ha-Mstn was expressed at lower levels in deep abdominal muscles than in CT and CR muscles. In intermolt animals, Ha-Mstn mRNA level in the DA muscle was significantly lower than the levels in both claw muscles (Fig. 5). Intermolt DA muscle Ha-Mstn levels were 67% lower than in CR muscle and 53% lower than in CT muscle. Although the means of the Ha-Mstn mRNA levels in DA muscle were also lower than the means in the claw muscles at premolt or postmolt stages, the mean differences were not statistically significant.

Removal of the X-organ/sinus gland, located within the eyestalk, induces precocious molting in *H. americanus* by removing the primary source of molt-inhibiting hormone (Chang and Bruce, 1980; Mauviot

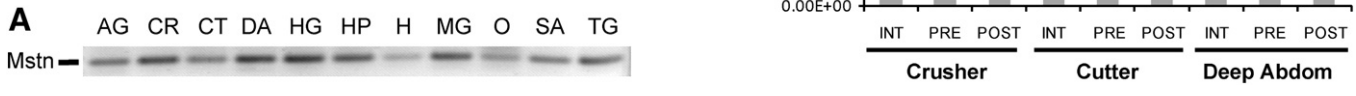

Fig. 4. Qualitative expression of myostatin (Ha-Mstn) in lobster tissues using end-point RT-PCR. Ha-EF2 (229 bp product), which served as a constitutively-expressed control, was expressed at similar levels in all tissues. Ha-Mstn (175 bp product) was expressed at apparently variable levels in all tissues. Abbreviations: AG, antennal gland; CR, crusher claw closer muscle; CT, cutter claw closer muscle; DA, deep abdominal muscle; H, heart; HG, hindgut; HP, hepatopancreas; MG, midgut; O, ovary; SA, superficial abdominal; and TG, thoracic ganglion. Representative inverse image of an ethidum bromide-stained agarose gel (RT-PCR and gel repeated 3 times).

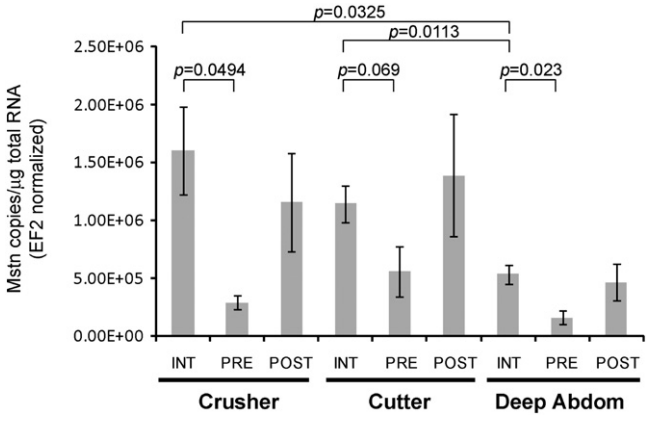

Fig. 5. Effects of molting on expression of Ha-Mstn. Ha-Mstn mRNA levels were quantified in cutter (CT; fast fibers) and crusher (CR; S_1 fibers) claw closer muscles and deep abdominal (DA; fast fibers) muscle from intermolt (INT), late premolt (PRE), or postmolt (POST) animals using qPCR. Data are expressed as copies of Ha-Mstn/μg total RNA, normalized according to Ha-EF2 copy numbers in the same samples (see Materials and methods; n = 6 for intermolt, 4 for late premolt, and 3 for postmolt). Significant differences between sample means were noted in Ha-Mstn; the means for Ha-EF2 expression were not significantly different. P values for differences between groups are indicated in the graph. There was a significant decrease in Ha-Mstn mRNA levels in CR and DA muscles from INT to PRE; however, the apparent decrease in CT muscle was not significant. In addition, the mean intermolt Ha-Mstn mRNA levels were significantly lower in DA muscle than in CR or CT muscles. No other significant differences were found.

and Castell, 1976; Skinner, 1985). We used this method, known as eyestalk ablation (ESA), to determine the response of intermolt animals to acute activation of the molting gland. As expected, ESA resulted in a large increase in hemolymph ecdysteroid concentrations at 7 days and 22 days post-ESA (Fig. 6B). The levels of Ha-Mstn and Ha-EF2 mRNAs were quantified in muscles from intact intermolt (0 day), 7 days post-ESA, and 22 days post-ESA animals (Fig. 6). There was no significant effect of ESA on expression of Ha-Mstn (Fig. 6A) or Ha-EF2. The Ha-EF2 mRNA levels (transcript copy number/μg total RNA) were as follows: $3.36 \pm 0.50 \times 10^7$ for Day 7 CR and $1.82 \pm 0.49 \times 10^7 \pm 4.86$ for Day 22 CR; $7.09 \pm 3.33 \times 10^6$ for Day 7 CT and $2.12 \pm 1.52 \times 10^7$ for Day 22 CT; and $2.99 \pm 1.41 \times 10^7$ for Day 7 DA and $3.18 \pm 1.02 \times 10^7$ for Day 22 DA. Furthermore, there was only a weak negative correlation ($r^2 = 0.0702$, Fig. 6C) of Ha-Mstn mRNA as a function of ecdysteroid concentration that was not statistically significant ($p = 0.25$). Expression of Ha-EF2 was also not correlated with ecdysteroid concentration (data not shown).

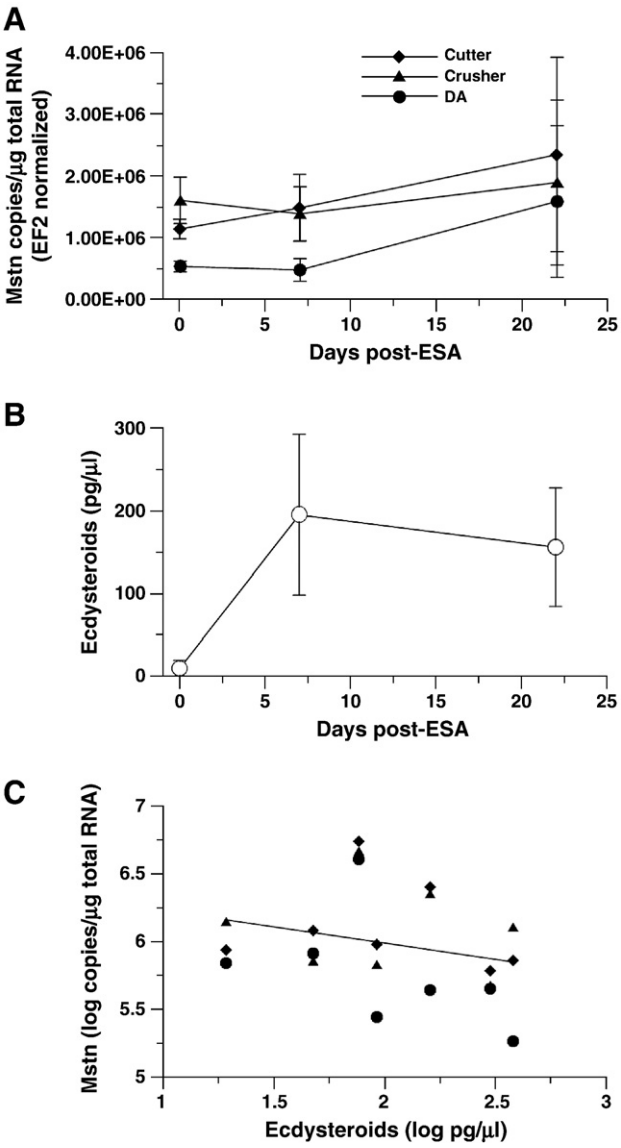

Fig. 6. Effects of eyestalk ablation (ESA) on Ha-Mstn mRNA and hemolymph ecdysteroid levels. (A) Ha-Mstn mRNA levels were quantified in cutter (CT; fast fibers) and crusher (CR; S_1 fibers) claw closer muscles and deep abdominal (DA; fast fibers) muscle from intact intermolt (Day 0) and eyestalk-ablated animals (7 and 22 days post-ESA) using qPCR. Data are expressed as copies of Ha-Mstn/μg total RNA, normalized according to Ha-EF2 copy numbers in the same samples (see Materials and methods; $n = 6$ for Day 0, same samples as INT in Fig. 5; $n = 3$ for Day 7 post-ESA; and $n = 3$ for Day 22 post-ESA). There was no significant effect of ESA on Ha-Mstn expression. (B) Hemolymph ecdysteroid levels, presented as mean ± 1 S.E., in intact (Day 0, $n = 6$) and eyestalk-ablated animals (Days 7 and 22; $n = 3$ for each). (C) Log Ha-Mstn mRNA copy number as a function of log hemolymph ecdysteroid concentration. There was no significant correlation for the combined data from all three muscles ($r^2 = 0.0702$; $p = 0.25$) or for data from each muscle separately ($r^2 = 0.0351$ and $p = 0.68$ for cutter claw muscle; $r^2 = 0.245$ and $p = 0.29$ for deep abdominal muscle; and $r^2 = 0.0285$ and $p = 0.72$ for crusher claw muscle). Symbols same as in part (A).

4. Discussion

Mstn, an important regulator of muscle growth and maintenance in higher vertebrates, has recently been shown to be present in lower vertebrates and invertebrates. We isolated the Mstn gene for the American lobster, *H. americanus*, from mixed muscle tissue RNA. It is the first astacuran Mstn cDNA to be cloned. Examination of the protein sequence by pairwise and multiple sequence alignment (Fig. 2) showed the greatest identities with the blackback land crab and Chinese mitten crab Mstn sequences. Comparing the relationship of the Mstn MP sequence with other invertebrate species within a rooted dendrogram (Fig. 3), the lobster sequence clustered with the other known Mstn-like genes and showed in particular the relatedness of this sequence to other decapod crustacean Mstn genes, firmly establishing the encoded protein as a Mstn-like member of the TGF-β family. The phylogenetic analysis (Fig. 3) identified a previously uncharacterized EST encoding a Mstn-like protein from Pacific white shrimp (*L. vannamei*). The Ha-Mstn sequence has the 9 cysteines and the furin cleavage site (Fig. 2) characteristic of vertebrate myostatins and inhibins (reviewed by Dominique and Gerard, 2006 and Lee, 2004), confirming that Ha-Mstn is a Mstn-like gene in lobster. Unlike mammals, in which Mstn is expressed primarily in skeletal muscle, crustacean Mstn is expressed at apparently varying levels in all tissues examined in lobster (Fig. 4) and land crab (Covi et al., 2008).

Homology modeling showed that the predicted three-dimensional structure of Ha-Mstn is similar to mammalian Mstn. The Ha-Mstn MP sequence was threaded through a crystal structure of mouse GDF-8 (=Mstn) homodimer bound to its inhibitor follistatin (Fst) (Cash et al., 2009) using the SWISS-MODEL Workspace (Fig. 7). The figure shows two molecules of Ha-Mstn MP surrounded by two molecules of Hs-Fst288 (Fig. 7A). There are no apparent conflicts in side chain binding in the overall protein structure, either within the Mstn homodimer or between the homodimer and follistatin. Indeed, a Ramachandran plot (Fig. 7B) shows that only one residue is found within an unfavorable region of the plot, indicating no unusual dihedral angles in the protein structure. The polypeptide backbones of the Ha-Mstn (one MP depicted in red; the other MP depicted in blue) and mouse GDF-8 (yellow) overlap nearly perfectly, except for a slightly longer loop in the Ha-Mstn adjacent to the α-helix (Fig. 7A, arrows). Perhaps not surprisingly, this loop region is located in a region of divergence within myostatins and does not interact with Fst (Fig. 2, asterisk; Covi et al., 2008). In addition, the residues important for binding of the N-terminal domain of Fst to Mstn (Cash et al., 2009) are highly conserved and consistent with the murine structure (Fig. 7C). The predicted backbone hydrogen bonding between Fst and Mstn in this region appears favorable (L16 to A54 in Ha-Mstn compared with L16 to L52 in mouse). The side chains of V15 and L16 in the nearby portion of Hs-Fst288[C] are able to fit easily in the crevice containing the prehelix loop region of Ha-Mstn[B] and contain residues of similar size to those in the murine sequence (49-FVFL-52 in mouse corresponds with 51-FLYA-54 in lobster). Hydrophobic interactions between side chains in the prehelix loop region of Mstn (murine F49 and V50) and the α-helix of the N-terminal domain of Fst288 (L46, F47, M50, and I51) appear possible in Ha-Mstn (F51 and L52), allowing close association between the two molecules. Furthermore, interactions with the N-terminal domain of Fst288 may be further stabilized by A58 and K65 of the lobster sequence, perhaps to a greater degree than the P56 side chain found in mouse Mstn. Although no Fsts

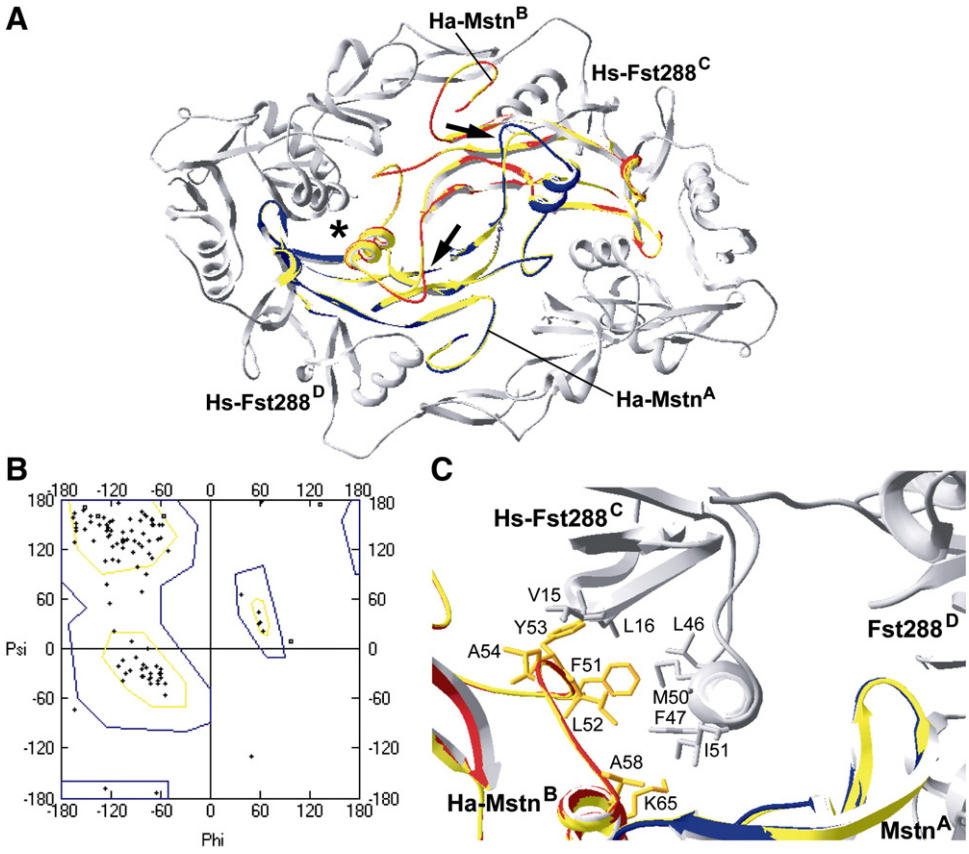

Fig. 7. Three-dimensional structural model of the mature peptide homodimer of lobster myostatin bound to its inhibitor follistatin. Using SWISS-MODEL Workspace (Arnold et al., 2006) a hypothetical structure of lobster myostatin, based on the crystal structure of mouse GDF-8 bound to human follistatin (Cash et al., 2009; structure 3hh2 at PDB, http://dx.doi.org/10.2210/pdb3hh2/pdb), was generated and visualized using DeepView 4.0.1 (Guex et al., 2009). The sequences showed 51% identity, and the alignment of the two sequences had an E value of 2.4×10^{-29}. The model of the Ha-Mstn homodimer bound to two molecules of human follistatin (A) had a total energy of -4370.876 kJ/mol and displayed only one unexpected amino acid in an unfavorable region when examined in a Ramachandran plot (B). In (A) Ha-Mstn monomer B (Ha-Mstn^B) is shown in red with the overlapping mouse GDF-8 underneath shown in yellow. Ha-Mstn^A is shown in blue, with the underlying GDF-8 also in yellow. Both molecules of human follistatin isoform 288 (Hs-Fst288^C and Fst288^D) are shown in gray. Arrows indicate loops (region indicated by * in Fig. 2) in Ha-Mstn (red/blue) that are slightly longer than the corresponding mouse GDF-8 (yellow). (C) Higher magnification of the interaction between Ha-Mstn and human Fst288. Colors are the same as in (A). The asterisk shown in (A) indicates the approximate region of the molecules shown in (C), with side chains of residues from Hs-Fst288^C and Ha-Mstn^B α-helices and loops visible in (C). The visual field shown in (C) is found by looking in the area of the asterisk from behind the molecules shown in (A) down the barrel of the Hs-Fst288^C N-terminal domain alpha helix. Side chains for residues thought to be involved in binding are shown, with numbers for Ha-Mstn residue numbers based on the MP sequence shown in bold italics in Fig. 1 (compare with Cash et al., 2009, Fig. 6D).

have yet been cloned from crustaceans, *Drosophila* expresses a Fst-like protein (Dm-Fst) that inhibits activin-mediated signaling during development (Pentek et al., 2009). Co-expression of Dm-Fst and myoglianin (the *Drosophila* Mstn ortholog) reduces pupal lethality caused by over-expression of Dm-Fst alone (Pentek et al., 2009), suggesting that myoglianin is an endogenous ligand of Dm-Fst. The structural model of Ha-Mstn and Hs-Fst288 indicates that mammalian Fst, which is commercially available, could be an effective reagent for the study of this pathway in crustacean muscles.

Given the importance of Mstn in growth and maintenance of vertebrate muscles (Lee and McPherron, 2001; McPherron et al., 1997; Rodgers and Garikipati, 2008), the ability of Mstn to regulate molt-induced claw muscle atrophy in crustaceans is a question of great interest. In *G. lateralis*, there is a dramatic down regulation of Gl-Mstn that coincides with a large increase in global protein synthesis, suggesting that Mstn suppresses translation (Covi et al., 2010). When molting is induced by either ESA or multiple limb autotomy (MLA; reviewed in Mykles, 2001; Skinner, 1985), premolt Gl-Mstn levels in claw muscle decrease 81% (ESA) or 94% (MLA), with 68% and 82% decreases, respectively, in thoracic muscle (Covi et al., 2010). The effects of molting on Mstn expression are comparable in lobster and land crab, when comparing muscles with the same fiber type composition. The claw closer muscle in *G. lateralis* is composed mostly of slow-twitch (S_1) fibers (Mykles, 1988; Mykles and Skinner, 1981). Ha-Mstn expression in the S_1 fibers of the CR muscle is reduced 82% in late premolt animals (Fig. 5). However, unlike land crabs, ESA had no significant effect on Ha-Mstn expression in intermolt lobsters. There was no change in Ha-Mstn mRNA levels at 7 or 22 days post-ESA in any muscle (Fig. 6A), and there was no correlation of Ha-Mstn mRNA levels with hemolymph ecdysteroid concentration (Fig. 6C). By contrast, Gl-Mstn mRNA levels in the land crab is negatively correlated with hemolymph ecdysteroid concentration (Covi et al., 2010). From these data, it appears that the transcription of Mstn in lobster muscles is less responsive to an acute increase in molting hormones than land crab muscles. The relative contribution of posttranslational regulation of Mstn may also differ in the two species. Altered processing of the Mstn protein occurs in mice and hamster cells (McMahon et al., 2003; Wolfman et al., 2003). Alternatively, changes in the expression of Mstn signaling proteins, such as activin receptors and Smad transcription factors, may play a greater role in regulating Mstn function in the lobster.

The three lobster muscles differed in Ha-Mstn expression. Molting has a differential effect on Ha-Mstn expression in fast and S_1 fibers (Fig. 5). Ha-Mstn mRNA decreased 82% in the S_1 fibers of the CR muscle, whereas the decreases were less in the fast fibers in the CT muscle (51%) and DA muscle (69%). Interestingly, the S_1 fibers in the

claws of land and fiddler crabs atrophy to a greater extent than the S_2 fibers (Ismail and Mykles, 1992; Mykles, 1997). The differences in the Ha-Mstn mRNA levels between the DA muscle and claw closer muscles in intermolt animals are not correlated with fiber type, however, as the fast fibers in the CT muscle expressed Ha-Mstn at significantly higher levels than the fast fibers in the DA muscle (Fig. 6). Taken together, the data indicate that the slow-twitch (S_1) fibers in the major claws of decapod crustaceans are more responsive to the atrophic signal.

In summary, a cDNA encoding a Mstn-like protein from an astacuran decapod was cloned and characterized. The conservation of the primary sequence and structural model (Fig. 7) indicates that the protein is processed and can fold in the same manner as mammalian myostatins. In brief, the Mstn MP is cleaved from the propeptide by furin and forms a homodimer stabilized by 8 intramolecular disulfide bridges (4 in each MP) and 1 intermolecular disulfide bridge (reviewed by Herpin et al., 2004; Lee, 2004). Mstn is transcriptionally regulated in lobsters, at least during the natural molt cycle, and resembles the overall pattern of Mstn expression in land crabs induced by MLA (Covi et al., 2010). The greater effect of molting on Ha-Mstn expression in CR muscle is consistent with the preferential atrophy of S_1 fibers in land and fiddler crabs (Ismail and Mykles, 1992; Mykles, 1997). However, unlike land crab (Covi et al., 2010), Ha-Mstn expression in intermolt lobster muscles appears refractory to an acute increase in circulating ecdysteroids caused by ESA. Mstn may play an important role in molt-induced muscle atrophy in lobsters, perhaps as an inhibitor of protein synthesis. In land crab, Gl-Mstn expression and protein synthesis are inversely correlated (Covi et al., 2010). The large down regulation of Ha-Mstn suggests that S_1 fibers in the crusher muscle undergo structural remodeling during premolt, which is facilitated by increasing protein turnover (Covi et al., 2010; Mykles, 1997). The effect of molting on Mstn expression is similar in a brachyuran (*G. lateralis*) and an astacuran (*H. americanus*), indicating that the transcriptional regulatory mechanism is conserved in decapod crustaceans.

Acknowledgements

The authors thank Stephanie Hjelmfelt, Matt Stratton, Lisa Axtman, Katie Regelson, and Moriah Echlin for assistance with cloning and expression and Sharon A. Chang for measuring ecdysteroids by radioimmunoassay. This study was funded by NSF grant lOS-0618203.

References

Aiken, D.E., 1973. Proecdysis, setal development, and molt prediction in the American lobster (*Homarus americanus*). J. Fish. Res. Board Can. 30, 1337–1344.
Arnold, K., Bordoli, L., Kopp, J., Schwede, T., 2006. The SWISS-MODEL workspace: a web-based environment for protein structure homology modelling. Bioinformatics 22, 195–201.
Carlson, C.J., Booth, F.W., Gordon, S.E., 1999. Skeletal muscle myostatin mRNA expression is fiber-type specific and increases dining hindlimb unloading. Am. J. Physiol. 277, R601–R606.
Cash, J.N., Rejon, C.A., McPherron, A.C., Bernard, D.J., Thompson, T.B., 2009. The structure of myostatin: follistatin 288: insights into receptor utilization and heparin binding. EMBO J. 28, 2662–2676.
Chang, E.S., Bruce, M.J., 1980. Ecdysteroid titers of juvenile lobsters following molt induction. J. Exp. Zool. 214, 157–160.
Chang, E.S., Conklin, D.E., 1983. Lobster (*Homarus*) hatchery techniques. In: McVey, J.P. (Ed.), CRC Handbook of Mariculture. CRC Press, Boca Raton, FL, pp. 271–275.
Chang, E.S., O'Connor, J.D., 1979. Arthropod molting hormones. In: Jaffe, B.M., Behrman, H.R. (Eds.), Methods of Hormone Radioimmunoassay. Academic Press, New York, pp. 797–814.
Chao, E., Kim, H.-W., Mykles, D.L., 2010. Cloning and tissue expression of eleven troponin-C isoforms in the American lobster, *Homarus americanus*. Comp. Biochem. Physiol. B 157, 88–101.
Conklin, D.E., Chang, E.S., 1983. Grow-out techniques for the American lobster, *Homarus americanus*. In: McVey, J.P. (Ed.), CRC Handbook of Mariculture. CRC Press, Boca Raton, FL, pp. 277–286.
Covi, J.A., Kim, H.W., Mykles, D.L., 2008. Expression of alternatively spliced transcripts for a myostatin-like protein in the blackback land crab, *Gecarcinus lateralis*. Comp. Biochem. Physiol. A 150, 423–430.
Covi, J.A., Bader, B.D., Chang, E.S., Mykles, D.L., 2010. Molt cycle regulation of protein synthesis in skeletal muscle of the blackback land crab, *Gecarcinus lateralis*, and the differential expression of a myostatin-like factor during atrophy induced by molting or unweighting. J. Exp. Biol. 213, 172–183.
Dominique, J.E., Gerard, C., 2006. Myostatin regulation of muscle development: molecular basis, natural mutations, physiopathological aspects. Exp. Cell Res. 312, 2401–2414.
Foster, K., Graham, I.R., Otto, A., Foster, H., Trollet, C., Yaworsky, P.J., Walsh, F.S., Bickham, D., Curtin, N.A., Kawar, S.L., Patel, K., Dickson, G., 2009. Adeno-associated virus-8-mediated intravenous transfer of myostatin propeptide leads to systemic functional improvements of slow but not fast muscle. Rejuven. Res. 12, 85–93.
Girgenrath, S., Song, K., Whittemore, L.A., 2005. Loss of myostatin expression alters fiber-type distribution and expression of myosin heavy chain isoforms in slow- and fast-type skeletal muscle. Muscle Nerve 31, 34–40.
Govind, C.K., 1992. Claw asymmetry in lobsters: case study in developmental neuroethology. J. Neurobiol. 23, 1423–1445.
Griffis, B., Moffett, S.B., Cooper, R.L., 2001. Muscle phenotype remains unaltered after limb autotomy and unloading. J. Exp. Zool. 289, 10–22.
Guex, N., Peitsch, M.C., Schwede, T., 2009. Automated comparative protein structure modeling with SWISS-MODEL and Swiss-PdbViewer: a historical perspective. Electrophoresis 30, S162–S173.
Hadjipavlou, G., Matika, O., Clop, A., Bishop, S.C., 2008. Two single nucleotide polymorphisms in the myostatin (GDF8) gene have significant association with muscle depth of commercial Charollais sheep. Anim. Genet. 39, 346–353.
Hennebry, A., Berry, C., Siriett, V., O'Callaghan, P., Chau, L., Watson, T., Sharma, M., Kambadur, R., 2009. Myostatin regulates fiber-type composition of skeletal muscle by regulating MEF2 and MyoD gene expression. Am. J. Physiol. 296, C525–C534.
Herpin, A., Lelong, C., Favrel, P., 2004. Transforming growth factor-beta-related proteins: an ancestral and widespread superfamily of cytokines in metazoans. Dev. Comp. Immunol. 28, 461–485.
Herrick, F.H., 1895. The American lobster. A study of its habits and development. Bull. U. S. Fish. Comm. 15, 1–252.
Ismail, S.Z.M., Mykles, D.L., 1992. Differential molt-induced atrophy in the dimorphic claws of male fiddler crabs, *Uca pugnax*. J. Exp. Zool. 263, 18–31.
Kim, H.W., Mykles, D.L., Goetz, F.W., Roberts, S.B., 2004. Characterization of a myostatin-like gene from the bay scallop, *Argopecten irradians*. Biochim. Biophys. Acta 1679, 174–179.
Kim, K.-S., Jeon, J.-M., Kim, H.-W., 2009. A myostatin-like gene expressed highly in the muscle tissue of Chinese mitten crab, *Eriocheir sinensis*. Fish. Aquat. Sci. 12, 185–193.
Kollias, H.D., McDermott, J.C., 2008. Transforming growth factor-beta and myostatin signaling in skeletal muscle. J. Appl. Physiol. 104, 579–587.
Lee, S.J., 2004. Regulation of muscle mass by myostatin. Annu. Rev. Cell Dev. Biol. 20, 61–86.
Lee, S.J., McPherron, A.C., 2001. Regulation of myostatin activity and muscle growth. Proc. Natl Acad. Sci. USA 98, 9306–9311.
Lo, P.C.H., Frasch, M., 1999. Sequence and expression of myoglianin, a novel *Drosophila* gene of the TGF-β superfamily. Mech. Dev. 86, 171–175.
MacDonald, C.C., Redondo, J.L., 2002. Reexamining the polyadenylation signal: were we wrong about AAUAAA? Mol. Cell. Endocrinol. 190, 1–8.
Matsakas, A., Patel, K., 2009. Intracellular signalling pathways regulating the adaptation of skeletal muscle to exercise and nutritional changes. Histol. Histopathol. 24, 209–222.
Matsakas, A., Foster, K., Otto, A., Macharia, R., Elashry, M.I., Feist, S., Graham, I., Foster, H., Yaworsky, P., Walsh, F., Dickson, G., Patel, K., 2009. Molecular, cellular and physiological investigation of myostatin propeptide-mediated muscle growth in adult mice. Neuromuscle Disord. 19, 489–499.
Mauviot, J.C., Castell, J.D., 1976. Molt-enhancing and growth-enhancing effects of bilateral eyestalk ablation on juvenile and adult American lobsters (*Homarus americanus*). J. Fish. Res. Board. Can. 33, 1922–1929.
McMahon, C.D., Popovic, L., Jeanplong, F., Oldham, J.M., Kirk, S.P., Osepchook, C.C., Wong, K.W.Y., Sharma, M., Kambadur, R., Bass, J.J., 2003. Sexual dimorphism is associated with decreased expression of processed myostatin in males. Am. J. Physiol. 284, E377–E381.
McPherron, A.C., Lee, S.J., 1997. Double muscling in cattle due to mutations in the myostatin gene. Proc. Natl Acad. Sci. USA 94, 12457–12461.
McPherron, A., Lawler, A., Lee, S., 1997. Regulation of skeletal muscle mass in mice by a new TGF-beta superfamily member. Nature 387, 83–90.
Medeiros, E.F., Phelps, M.P., Fuentes, F.D., Bradley, T.M., 2009. Overexpression of follistatin in trout stimulates increased muscling. Am. J. Physiol. 297, R235–R242.
Medler, S., Mykles, D.L., 2003. Analysis of myofibrillar proteins and transcripts in adult skeletal muscles of the American lobster *Homarus americanus*: variable expression of myosins, actin and troponins in fast, slow-twitch and slow-tonic fibres. J. Exp. Biol. 206, 3557–3567.
Medler, S., Lilley, T.R., Riehl, J.H., Mulder, E.P., Chang, E.S., Mykles, D.L., 2007. Myofibrillar gene expression in differentiating lobster claw muscles. J. Exp. Zool. 307A, 281–295.
Mendias, C.L., Marcin, J.E., Calerdon, D.R., Faulkner, J.A., 2006. Contractile properties of EDL and soleus muscles of myostatin-deficient mice. J. Appl. Physiol. 101, 898–905.
Mosher, D.S., Quignon, P., Bustamante, C.D., Sutter, N.B., Mellersh, C.S., Parker, H.G., Ostrander, E.A., 2007. A mutation in the myostatin gene increases muscle mass and enhances racing performance in heterozygote dogs. PLoS Genet. 3, 779–786.
Mykles, D.L., 1985. Multiple variants of myofibrillar proteins in single fibers of lobster claw muscles: evidence for two types of slow fibers in the cutter closer muscle. Biol. Bull. 169, 476–483.
Mykles, D.L., 1988. Histochemical and biochemical characterization of two slow fiber types in decapod crustacean muscles. J. Exp. Zool. 245, 232–243.
Mykles, D.L., 1997. Crustacean muscle plasticity: Molecular mechanisms determining mass and contractile properties. Comp. Biochem. Physiol. B 117, 367–378.

Mykles, D.L., 2001. Interactions between limb regeneration and molting in decapod crustaceans. Am. Zool. 41, 399–406.
Mykles, D.L., Skinner, D.M., 1981. Preferential loss of thin filaments during molt-induced atrophy in crab claw muscle. J. Ultrastruct. Res. 75, 314–325.
Mykles, D.L., Skinner, D.M., 1982a. Crustacean muscles: atrophy and regeneration during molting. In: Twarog, B.M., Levine, R.J.C., Dewey, M.M. (Eds.), Basic Biology of Muscles: A Comparative Approach. Raven Press, New York, pp. 337–357.
Mykles, D.L., Skinner, D.M., 1982b. Molt cycle-associated changes in calcium-dependent proteinase activity that degrades actin and myosin in crustacean muscle. Dev. Biol. 92, 386–397.
Page, R.D.M., 1996. TreeView: an application to display phylogenetic trees on personal computers. Comput. Appl. Biosci. 12, 357–358.
Patruno, M., Caliaro, F., Maccatrozzo, L., Sacchetto, R., Martinello, T., Toniolo, L., Reggiani, C., Mascarello, F., 2008. Myostatin shows a specific expression pattern in pig skeletal and extraocular muscles during pre- and post-natal growth. Differentiation 76, 168–181.
Pentek, J., Parker, L., Wu, A., Arora, K., 2009. Follistatin preferentially antagonizes activin rather than BMP signaling in *Drosophila*. Genesis 47, 261–273.
Rodgers, B.D., Garikipati, D.K., 2008. Clinical, agricultural, and evolutionary biology of myostatin: a comparative review. Endocr. Rev. 29, 513–534.
Salerno, M.S., Thomas, M., Forbes, D., Watson, T., Kambadur, R., Sharma, M., 2004. Molecular analysis of fiber type-specific expression of murine myostatin promoter. Am. J. Physiol. 287, C1031–C1040.
Schmiege, D.L., Ridgway, R.L., Moffett, S.B., 1992. Ultrastructure of autotomy-induced atrophy of muscles in the crab *Carcinus maenas*. Can. J. Zool. 70, 841–851.
Skinner, D.M., 1965. Amino acid incorporation into protein during the molt cycle of the land crab, *Gecarcinus lateralis*. J. Exp. Zool. 160, 225–234.
Skinner, D.M., 1966. Breakdown and reformation of somatic muscle during the molt cycle of the land crab, *Gecarcinus lateralis*. J. Exp. Zool. 163, 115–124.
Skinner, D.M., 1985. Molting and regeneration. In: Bliss, D.E., Mantel, L.H. (Eds.), The Biology of Crustacea. Academic Press, New York, pp. 43–146.
Steelman, C.A., Recknor, J.C., Nettleton, D., Reecy, J.M., 2006. Transcriptional profiling of myostatin-knockout mice implicates Wnt signaling in postnatal skeletal muscle growth and hypertrophy. FASEB J. 20, 580–582.
Thompson, J.D., Gibson, T.J., Plewniak, F., Jeanmougin, F., Higgins, D.G., 1997. The CLUSTAL_X windows interface: flexible strategies for multiple sequence alignment aided by quality analysis tools. Nucleic Acids Res. 25, 4876–4882.
Tisdale, M.J., 2009. Mechanisms of cancer cachexia. Physiol. Rev. 89, 381–410.
Welle, S., Burgess, K., Thornton, C.A., Tawil, R., 2009. Relation between extent of myostatin depletion and muscle growth in mature mice. Am. J. Physiol. 297, E935–E940.
West, J.M., 1997. Ultrastructural and contractile activation properties of crustacean muscle fibres over the moult cycle. Comp. Biochem. Physiol. B 117, 333–345.
Wolfman, N.M., McPherron, A.C., Pappano, W.N., Davies, M.V., Song, K., Tomkinson, K.N., Wright, J.F., Zhao, L., Sebald, S.M., Greenspan, D.S., Leet, S.I., 2003. Activation of latent myostatin by the BMP-1/tolloid family of metalloproteinases. Proc. Natl Acad. Sci. USA 100, 15842–15846.
Ye, X.H., Brown, S.R., Nones, K., Coutinho, L.L., Dekkers, J.C.M., Lamont, S.J., 2007. Associations of myostatin gene polymorphisms with performance and mortality traits in broiler chickens. Genet. Sel. Evol. 39, 73–89.
Yu, X.L., Chang, E.S., Mykles, D.L., 2002. Characterization of limb autotomy factor-proecdysis (LAF_{pro}), isolated from limb regenerates, that suspends molting in the land crab *Gecarcinus lateralis*. Biol. Bull. 202, 204–212.